THE PHENIX PHYSICS PROGRAM AT RHIC

WILLIAM A. ZAJC

Department of Physics, Columbia University, NY, NY 10027, USA

The PHENIX detector is one of two large detectors being built for the Relativistic Heavy Ion Collider (RHIC) at Brookhaven National Laboratory. RHIC will provide colliding beams of relativistic (100 A $\cdot$ GeV) heavy ions as well as polarized protons at $\sqrt{s} = 500$ GeV. The physics capabilities of the PHENIX detector for the heavy ion portion of the RHIC program are briefly outlined here.

1 Introduction

Brookhaven's Relativistic Heavy Ion Collider (RHIC), which is on schedule for completion in 1999, will be a unique facility for exploring the hadronic structure of bulk nuclear matter. No other machine will be capable of accelerating such a broad range of species (protons to Au nuclei) to such high energies (maximum energy per beam of $\sim \frac{\mathrm{Z}}{\mathrm{A}} \cdot 250$ GeV) with such intense luminosities ($\sim 2\times 10^{26}$ cm^{-2} s^{-1} for Au-Au collisions). It is thought that collisions of the heaviest ions at the highest RHIC energies are the precise conditions necessary to form the quark-gluon plasma (QGP)[1]. Regardless of the new phenomena created at RHIC, the range of species and energies available from this machine provides the necessary ingredients for the systematic exploration required to establish that new physics has indeed been observed.

With such opportunities come immense experimental challenges. Experiments must be designed to accomodate extremely high particle densities ($\frac{dN}{dy} \sim$ 1000 at central rapidities), and from such events extract evidence for a phase transition in a highly transient environment. The energy dependence and especially the cross-section for plasma formation are completely unknown– guesstimates range from every central event to not at all! Signatures for the QGP are nearly as ambiguous, and none of them have the distinguishing feature of incontrovertibility. The best hope for progress appears to be the pursuit of many signals in parallel, as guided by previous heavy ion experience, appropriately modified for the new energy regime and observables attainable at RHIC. Since the both the formation rates and the persistence of signatures are unknown, it is essential to maintain the highest possible rate capability.

2 The PHENIX Experiment

PHENIX[2] is one of two large experiments at RHIC. The PHENIX approach to RHIC physics can be stated simply as: *Search for the "simultaneous" appearance of new phenomena in as many channels as possible, as a function of some "external" parameter.* Each of the quoted words warrants some explanation. "Simultaneous" does not necessarily mean in the same event. Instead, it implies that for some class of events, the various new phenomena appear at or near the *same* value of the "external" parameter. A few obvious candidates of the external parameter are:

- The *mass* of the colliding ions.
- The $\sqrt{s}$ of the colliding ions.
- The *energy density* of the collision.

These are not all independent quantities (for instance, it is likely that the energy density will grow with as $A^{1/3}$ and logarithmically with $\sqrt{s}$), so an important second-order goal will be establishing the "best" such external parameter.

Which channels[3] are likely to be of interest? A simple enumeration of potential signals quickly produces a rather extensive menu:

1. Deconfinement (Debye Screening)
   - $R(\Upsilon) \sim 0.13$ fm $< R(J/\psi) \sim 0.29$ fm $< R(\psi') \sim 0.56$ fm
     $\Rightarrow$ Electrons, Muons
2. Chiral Symmetry Restoration
   - Mass, width, branching ratio of $\phi \to e^+e^-$, K^+K^- with $\delta M \leq$ 5 MeV.
     $\Rightarrow$ Electrons, Muons, Charged Hadrons
   - Baryon susceptibility; color fluctuations: Anti-baryon production
     $\Rightarrow$ Charged Hadrons
   - DCC's: Isospin fluctuations
     $\Rightarrow$ Photons, Charged Hadrons
3. Thermal Radiation of Hot Gas
   - Prompt γ, Prompt $\gamma^* \to e^+e^-, \mu^+\mu^-$
     $\Rightarrow$ Photons, Electrons, Muons

4. Strangeness and Charm Production
   - Production of K^+, K^-, K^0_s mesons
     $\Rightarrow$ Hadrons
   - Production of ϕ, J/ψ, D mesons
     $\Rightarrow$ Electrons, Muons
5. Jet Quenching
   - High-p_T jet via leading particle spectra
     $\Rightarrow$ Hadrons, Photons
6. Space-Time Evolution
   - HBT Correlations of $\pi^\pm, \pi^\pm$, $K^\pm K^\pm$
     $\Rightarrow$ Hadrons

The conclusion, of course, is that is highly desirable to measure in one experiment electrons, muons, photons, and charged hadrons. Is it possible to measure this ambititious list of phenomena in central A-A collisions at RHIC in one detector (at finite cost)? The PHENIX answer to this question is "Yes" (if one measures over finite intervals).

The remainder of this manuscript will describe the PHENIX apparatus and the measurements made possible by it. Before proceeding, two items are worth noting. First, the capabilities of the PHENIX detector will allow measurement of "direct" probes such as charmonium and direct photons in conjunction with "event charecterization" data such as two-particle correlations and transverse energy. This is a unique capability, virtually absent from the existing fixed target heavy ion experiments, which have nonetheless (as a result?) generated some very provacative results. Second, the same virtues imposed on PHENIX by the RHIC heavy ion environment (e.g., very high granularity, high rate capability) provide a superb detector for pursuing spin physics at RHIC with beams of polarized protons. This wonderful complement to the heavy ion program is described elsewhere[4].

3 The PHENIX Apparatus

The PHENIX collaboration has chosen to measure electrons, photons and hadrons in the central region $|y| < 0.35$, and muons in the rapidity slice $1.2 < |y| < 2.5$. This approach results in a four-armed design, as shown in Figure 3, consisting of two central arms, each covering 90^o of azimuth, and two full-azimuth muon arms.

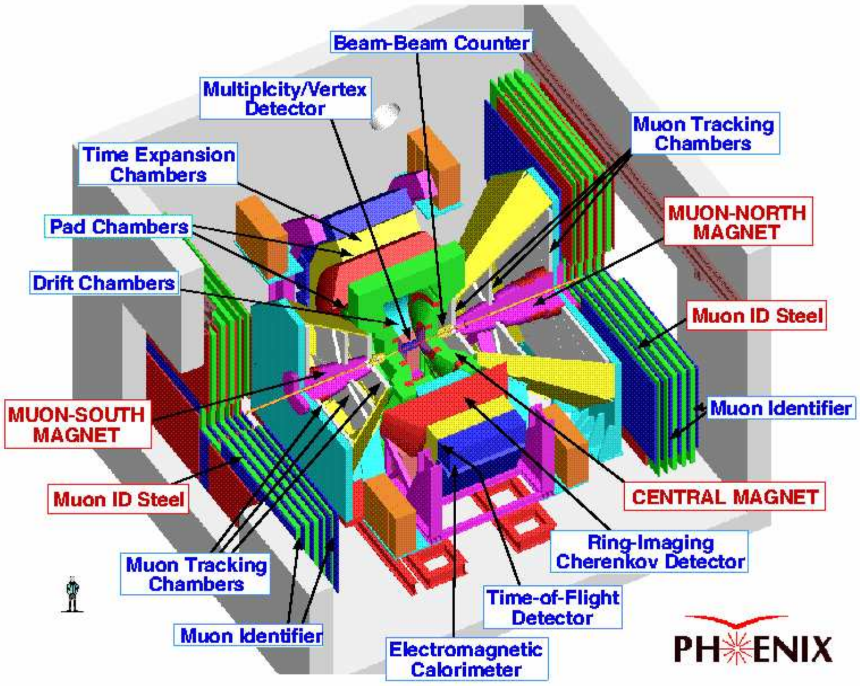

Figure 1: The PHENIX detector. The central detector arm on the far side of the detector is the West arm; the right-hand muon arm is the North arm.

The central magnet produces a roughly axial magnetic field in the central region for momentum analysis of charged particles. Each central arm contains three tracking sub-systems: The r-ϕ coordinate is measured in the drift chamber (DC) with one-sided drift cells to avoid left-right ambiguities; similar cells with small-angle stereo provide rough z measurements, Three layers of pixel pad chambers (PC1, 2 and 3) will determine space points on the trajectories, and provide the primary source of z information. A time-expansion chamber (TEC) provides both tracking and particle ID via dE/dx and transition radiation. PC1 and PC2 are separated by a $\sim$ 140 cm gas volume for the Ring Imaging Cerenkov (RICH) detector, which is read out by phototubes located on the magnet pole tips. The gas volume, filled with atmospheric pressure ethane ($\gamma_{th} \sim 25$), identifies electrons. The outermost detectors in the central arm are very finely segmented ($\Delta\eta \times \Delta\phi \sim 0.01 \times 0.01$) PbGl (West arm) and

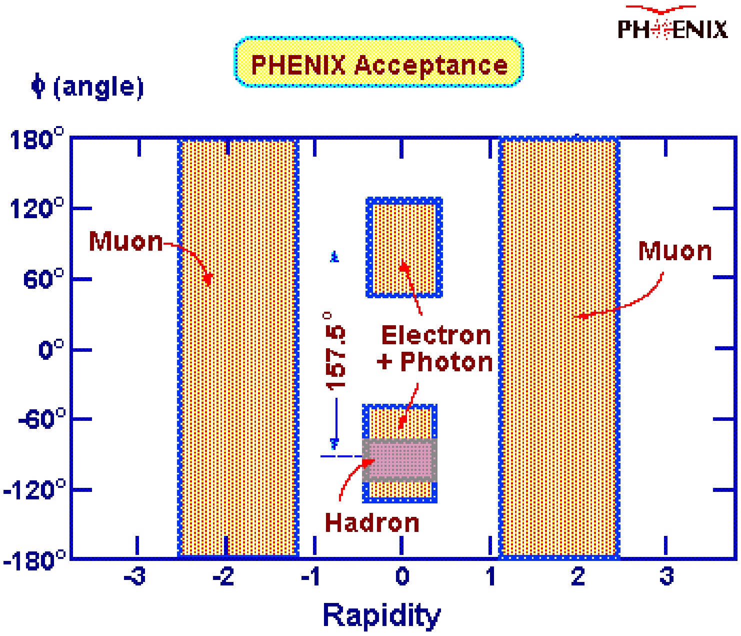

Figure 2: The acceptance regions of the PHENIX central and muon arms.

Pb-Scintillator (both arms) electromagnetic calorimeters for measuring photons and electrons. A precision ($\sigma_t \sim 80$ ps) time-of-flight array covering half the azimuth of the West arm will be used to identify charged hadrons in this aperture.

The two large conical structures apparent in Figure 3 are the North and South muon magnets, which (with the aid of a central cylindrical "pistons" produce a roughly radial magentic field. Muons in the angular range $10^o < \theta < 35^o$ are momentum analyzed in three stations of cathode strip chambers (CSC's). Identification of the muons is based on their penetration through up to five layers of steel absorber, which is interspersed with limited streamer tubes (LST's) for readout. It should be noted that an important "component" of the muon detection system is passive, namely, absorbers consisting of the central magnet steel and additional material, designed to absorb produced hadrons before their decays produce muons.

As stated in Section 2, the PHENIX approach to studying heavy ion collisions at RHIC relies on the correlation of many observables with respect to some "external" parameter. One such quantity is the total charged multiplicity measured in the region $|\eta| < 2.5$ by the Multiplicity Vertex Detector (MVD), which consists of Si strips and pads covering the full azimuth. The MVD also provides on-line determination of the vertex (used in higher-level triggering). Another important source of vertex information are the Beam-Beam (BB) counters, which consist of two arrays of 64 phototubes each, detecting relativistic charged particles via Cerenkov light in the interval $3 < |\eta| < 4$. These counters also provide the essential **START** time used in time-of-flight analysis.

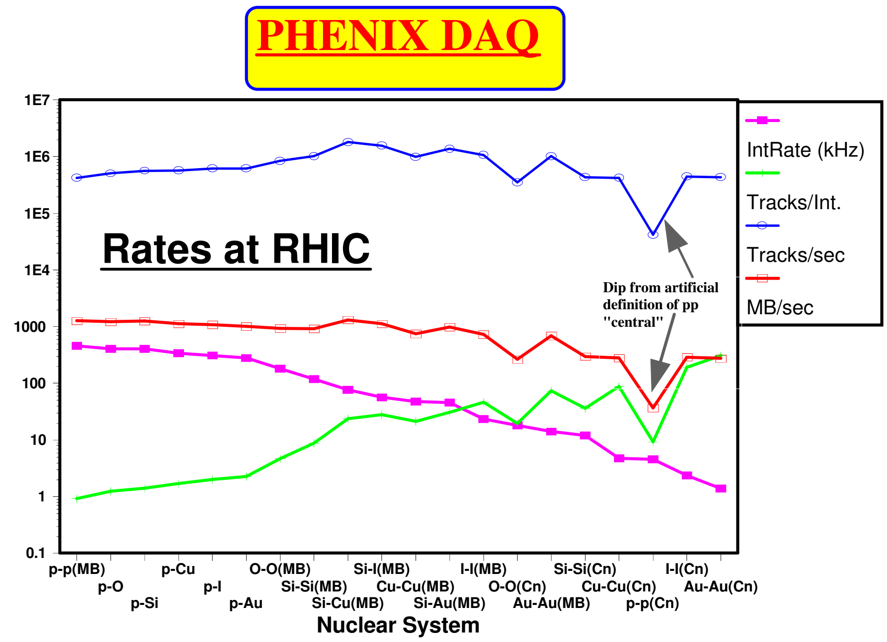

Figure 3: Collision rates and PHENIX data volumes at RHIC for (roughly) 10 times design luminosity.

As emphasized in Section 1, the lack of definitive cross-section predictions for QGP formation argues for building an experiment with the highest possible rate capabilities. The front end electronics (FEE), data acquisition (DAQ) and trigger systems of PHENIX have been designed to perform, for all colliding species, at luminosities an order-of-magnitude greater than the nominal design luminosity of RHIC. As shown in Figure 3, this is an extremely challenging task– while the rate at which data is produced in PHENIX is roughly independent of colliding species, the magnitude of this number is large ($\sim$ 2 GB/s). More importantly, the nature of the data varies from very small events occuring at very high rate (pp at $\sim$ 1 MHz) to very large events at small rate (central Au-Au at $\sim$ 1kHz). Regardless of species, the PHENIX FEE can read out the entire detector at a sustained rate of 25 kHz. Collision rates which exceed the input bandwidth of the system must be reduced by the Level-1 trigger; rates which exceed the ouput bandwidth of the system (20 MB/s) must be further reduced by higher-level triggers based on the physics content of the events.

4 PHENIX Physics

4.1 Low P_T Hadron Physics

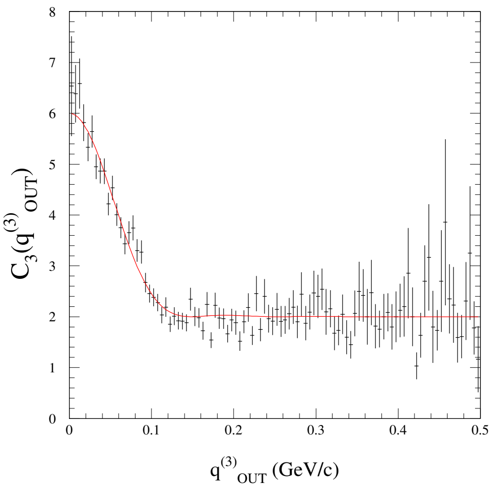

Figure 4: The three-pion correlation function for triplets from 10^5 central Au-Au events as measured in the PHENIX high-resolution hadron sector.

The tremendous data volumes implicit in Figure 3 are generated almost entirely by hadrons. This fact, together with the large apertures and sophisticated DAQ systems found in RHIC experiments, implies that measurements which normally require weeks in fixed-target programs can be made in days or even hours at RHIC. A good illustration of this is the rate for correlation physics, shown in Figure 4. There a *three*-pion correlation function for a source with longitudinal, outward and sideward radii $R_L = R_O = R_S = 6$ fm is shown as measured in the PHENIX aperture, for a greatly restricted subset of the three-particle phase space, namely all $q_L < \hbar/R_L$. and all $q_S < \hbar/R_S$. The resulting correlation function is then plotted versus the "out" component between particles 1 and 2. The data are for a simulation of 10^5 central Au-Au events; at design luminosity this corresponds to less than one hour of data-taking(!).

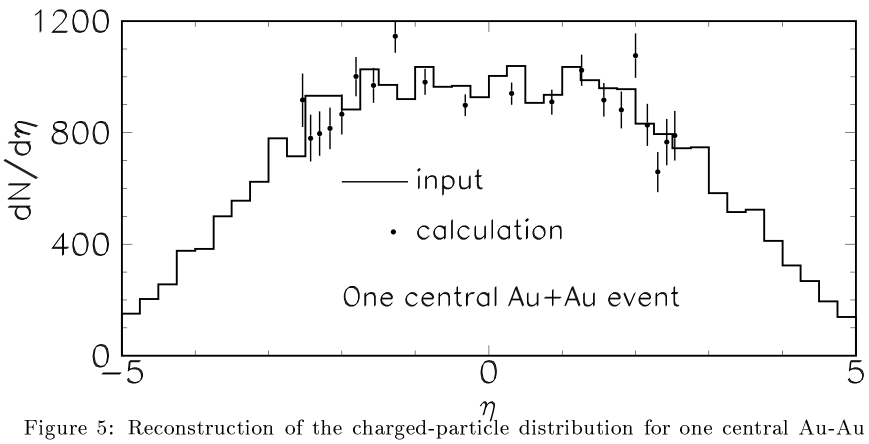

Figure 5: Reconstruction of the charged-particle distribution for one central Au-Au event using the Multiplicity Vertex Detector, versus the input distribution.

Recently much attention has been focused on an explicit indicator of a second-order phase transition that appears in the hadronic sector, the Disoriented Chiral Condensate (DCC)[5], which results in non-Poissonian fluctuations in the yield of charged and neutral pions (particularly at low transverse momenta). Due to its finely segmented EmCal, PHENIX has a unique ability to identify DCC's through their effect on the π^0 spectrum. For instance, fluctuations in the MVD's event-by-event reconstruction of the charged-particle pseudo-rapidity spectrum in the region $|\eta| < 2.5$ (Figure 5) can be correlated with the number of low-p_T clusters in the EmCal.

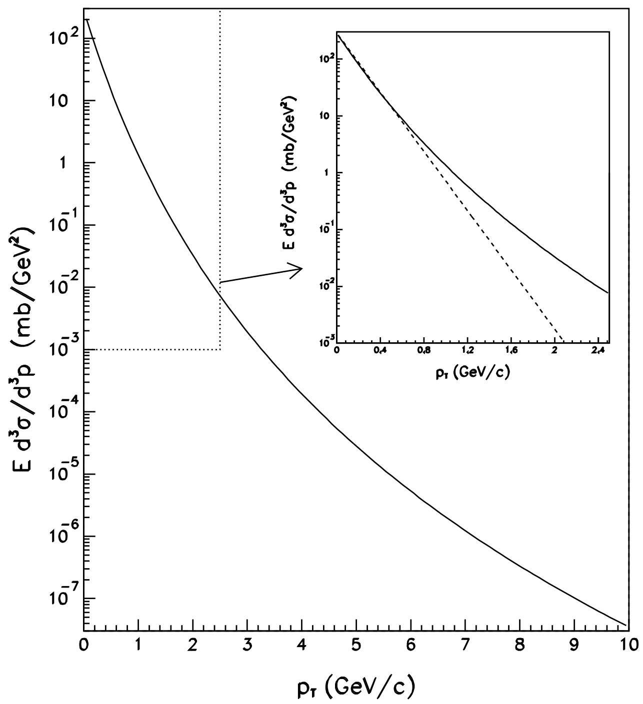

Figure 6: The expected (p-p) transverse momentum spectrum at RHIC energies. The inset provides an expanded view of the "low-p_T" region, compared to the usual soft exponential parameterization.

4.2 High P_T Hadron Physics

While hadron measurements at low transverse momenta are essential to understanding the bulk "freeze-out" behavior of the matter produced at RHIC, high p_T data provide complementary information on the hard dynamics at play in the initial stages of the collision. There is of course no rigorous dividing line between these two regimes, as shown in Figure 6, which shows the single-particle p_T spectrum expected at RHIC, parameterized as

$$\frac{dn}{dp_T^2} \sim \left(\frac{p_0}{p_0 + p_T}\right)^4 \quad , \tag{1}$$

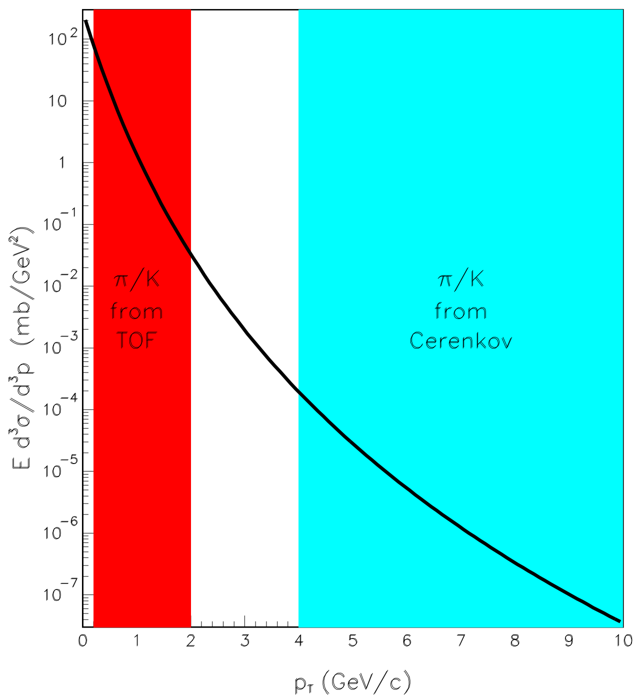

Figure 7: The Particle Identification regions for the PHENIX RICH detector.

with $p_O \sim 0.5$ GeV. The deviation from the soft, "$e^{-\alpha p_T}$" form is already apparent at transverse momenta of order 1 GeV/c. (This behavior is not surprising, since the dimensionful parameters in QCD are all of order Λ_{QCD}.)

It has long been known that the flavor composition of hadrons at large p_T is a probe of the underlying parton distributions. For example, at the ISR the Split Field Magnet Collaboration showed that high-p_T K^-'s are suppressed relative to K^+'s, since the K^- contains no valence quarks from the initial nucleons[6]. As shown in Figure 7, PHENIX will be able to cleanly identify high transverse momentum pions and kaons using the RICH detector. By using the precision time-of-flight detector, anti-protons are also measurable out to roughly 4 GeC/c. These too may be sensitive probes of the gluon distributions[7].

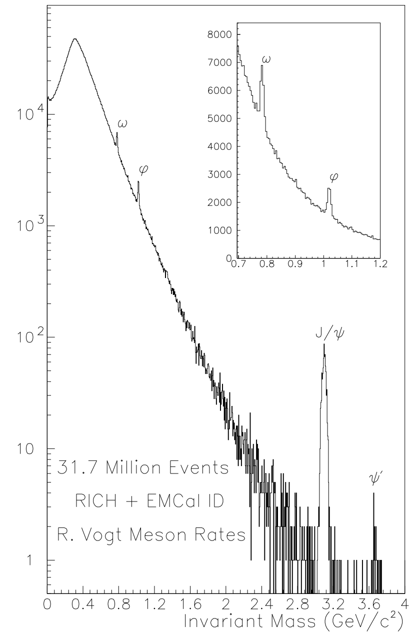

Figure 8: The dielectron pair mass spectrum expected in the PHENIX cental aperture from $\sim 3 \times 10^7$ events.

PHENIX has made a concerted effort to optimize the detectors in the central arms for electron and photon detection. Much of the interest centers on the decays of the vector mesons to electron pairs. Figure 8 (from the PHENIX Conceptual Design Report[8]) shows a dielectron mass spectrum for $\sim 3 \times 10^7$ central Au-Au events in the PHENIX central arms, with clear peaks above the combinatoric background containing several thousand ω's, a thousand ϕ's and and several hundred J/Ψ 's. (Since these mesons are produced hadronically, their abundances are large; the only reason these rates are "small" is the $\sim 10^{-4}$ branching ratio to e^+e^-.) In fact, the time to acquire $\sim 3 \times 10^7$ pairs is

- $\sim$ 10 weeks at $\frac{1}{100}$ design luminosity
- $\sim$ 1 week at $\frac{1}{10}$ design luminosity
- $\sim$ 1 week at design luminosity (without a trigger)

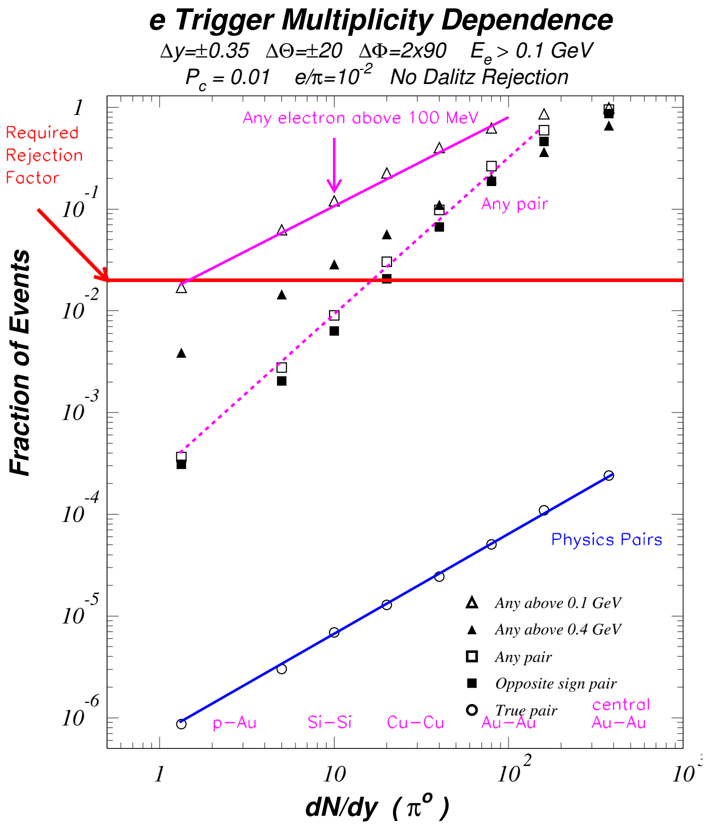

Figure 9: The fraction of events containing various electron signatures in the PHENIX aperture, as a function of the π^0 dN/dy.

- $\sim$ 1 week at 10$\times$ design luminosity (without a trigger)

That is, at design luminosity RHIC produces central Au-Au collisions at roughly an order-of-magnitude greater rate than PHENIX can accept. Clearly a trigger to select the "interesting" events is called for. It is absolutely inadequate to declare "interesting" as "having an e^+e^- pair", as shown in Figure 9, which plots the rejection factor available by triggering on electrons in the PHENIX

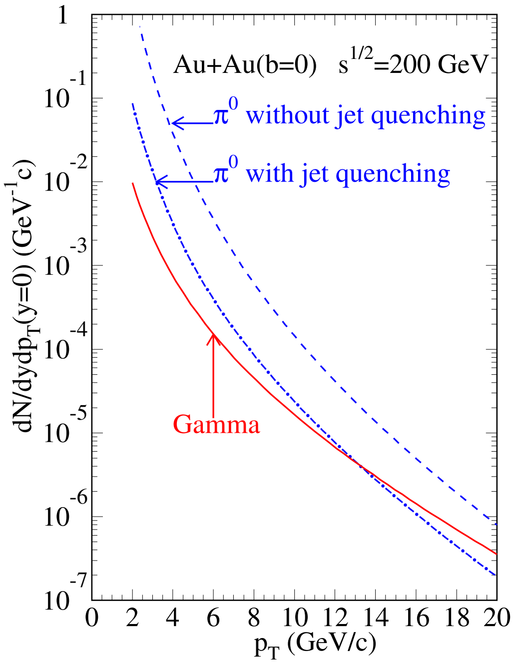

Figure 10: The direct photon spectrum for central Au-Au collisions versus the π^0 background with and without jet quenching[10].

aperture[9]. Since there are several such electrons per central Au-Au event, a more sophisticated strategy will be required to preserve DAQ bandwidth for comparatively rare J/Ψ 's. Such "physics-based" triggers are under active study at the moment, and will likely be implemented at Level-2.

4.4 Direct Photons

Direct photons are thought to be emitted copiously by the plasma, and escape the interacting matter with essentially no interaction. As such, they are in principle superb diagnostics of thermal history of the collision[11]. In practice, their experimental detection is extremely challenging, since the overwhelming background from hadronic decays (dominantly π^0's and η's) must first be measured and eliminated[12]. This requires a finely segmented electromagnetic calorimeter augmented with charged-particle tracking, as deployed in the PHENIX central arms. The precise details of determining π^0 and η yields as a function of multiplicity and transverse momentum are described elsewhere [2,8,13,14].

The very large combinatoric background at low transverse momentum is substantially reduced at higher p_T values. In fact, if there is substantial jet quenching the direct photon yield may even exceed the hadronic yield for $p_T >\sim 12$ GeV[10], as shown in Figure 10. Here we have the happy situation of one plasma signature (jet quenching[15]) helping another (direct photons). The only problem appears to be one of rate, and is not terribly serious: At design luminosities, the predicted yield at $p_T \sim 12$ GeV/c of $\frac{dN}{dy dp_T} \sim 10^{-5}$ GeV^{-1} gives a rate in the PHENIX aperture of one photon per hour (in a 1 GeV/c bin). This is a case where a trigger is straightforward, since the number of clusters in the EmCal with this energy per central Au-Au event is well below unity, so that live-time can be preserved by rejecting events not satisfying this condition. Correspondingly, the rate can be increased almost linearly by raising the luminosity above the design value. If such gains can be achieved, this opens up the exciting possibility of directly observing the effect of jet quenching on the fragmentation function by using the photon as a tag[16], and examining the particle distribution opposite to it.

4.5 Muons

Much of the physics discussed in Section 4.3 is also measured in the North and South muon arms. As shown in Figure 11, clear peaks for the various vector mesons emerge after a like-sign subtraction. Note in particular that the spectrum extends beyond $M_{\mu\mu} = 10$ GeV, which allows for measurement of the Υ. Due to its very small Bohr radius (~ 0.13 fm), measurement of the Υ should be instrumental in understanding the systematics of J/Ψ and ψ' suppression. The mass region between the J/Ψ and the Υ is dominated by open charm prodcution (see the next section). Table 1 demonstrates that the performance of the PHENIX muon systems compares very well[17] to the FNAL experiment E772, which has been a leader in exploring the production of heavy vector mesons in p-A collisions.

4.6 Charm

While the discussion of electron physics in Section 4.3 concentrated on measurement of the vector mesons, observed as peaks in the dilepton pair mass,

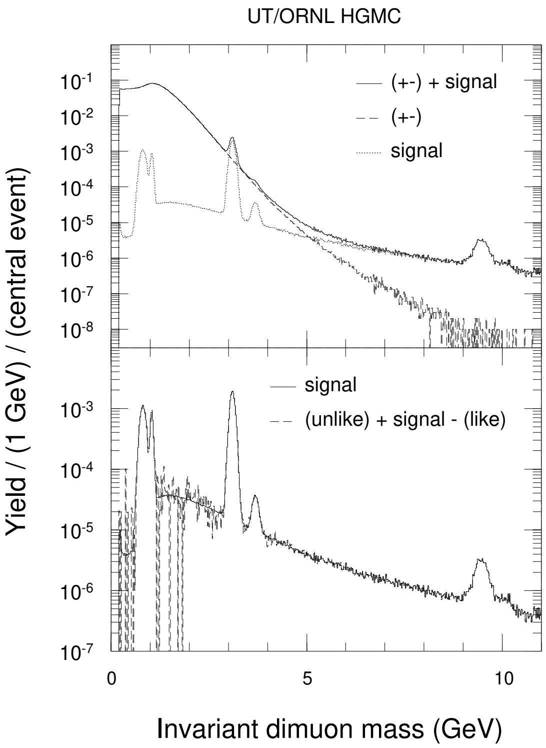

Figure 11: The PHENIX North Muon arm spectrum before and after subtraction of a like-sign combinatoric background.

there is also substantial interest in the dilepton continuum, since virtual photons, just as real ones, diagnose the thermal evolution of the plasma. The penalty in rate from the extra factor of α must be paid, but the enormous backgrounds from the π^0 and η that so affect the direct photon measurement are absent. This optimistic scenario led many researchers circa 1990 to advocate measurement of the thermal dileptons yield as a plasma probe.

Since then, it has become clear that dileptons *do* provide substantial information on the evolution of the interacting matter, but via the production of *open charm* rather than by thermal mechanisms[19]. That is, the thermal spectrum lies one to two orders-of-magnitude below the charm signal, as shown in Figure 4.6. (Ironically, even the lepton pairs in thermally produced charm exceeds the directly produced thermal dileptons.) This dominance of the charm signal has prompted several authors to suggest using it rather than thermal

Table 1: Comparison of some PHENIX muon performance to the fixed-target experiment E772 at Fermilab. The yields are calculated for 3000 hours of running[17].

	PHENIX Central Au + Au	PHENIX Min. bias Au + Au	FNAL E772
$\rho \to \mu^+ + \mu^-$	> 300K	> 1M	-
$\phi \to \mu^+ + \mu^-$	> 139K	> 500K	-
$J/\psi \to \mu^+ + \mu^-$	700K	3M	100K
$\psi' \to \mu^+ + \mu^-$	10K	24K	12K
$\Upsilon \to \mu^+ + \mu^-$	2160	9K	17K
D-Y (4-9 GeV)	$\sim$ 24K	$\sim$ 100K	450K
$\sqrt{s}$ (GeV)		200	39
x_F		-0.3 to 0.3	0 to 0.6
p_T (GeV)		0-10	0-2.5
x_2		$\sim 10^{-4}$-0.2	$\sim$ 0.03-0.27

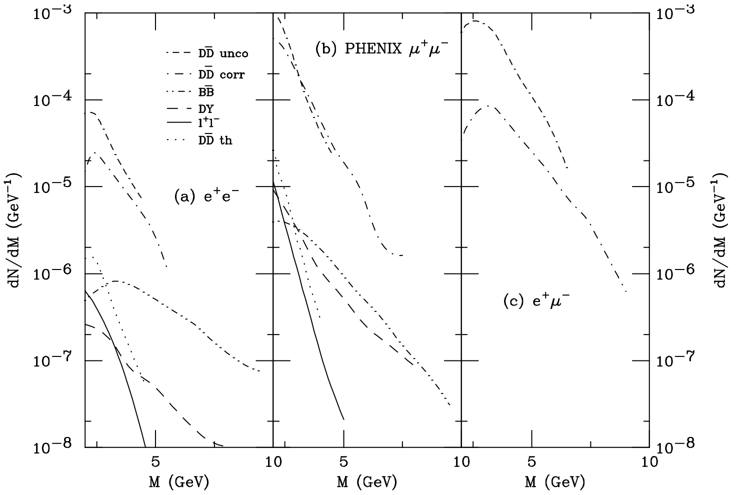

Figure 12: Contributions to the dilepton spectrum as measured in PHENIX. The "D $\bar{\text{D}}$ uncorr" curve is for dileptons originating from different c $\bar{\text{c}}$ pairs; "D $\bar{\text{D}}$ corr" curve is for dileptons originating from the same c $\bar{\text{c}}$ pair. (From Ref. 19.)

dileptons as the canonical probe of the initial densities[20,21,22].

Accumulating sufficient high-mass muon and electron pairs will be a relatively straightforward procedure for the PHENIX experiment, as indicated

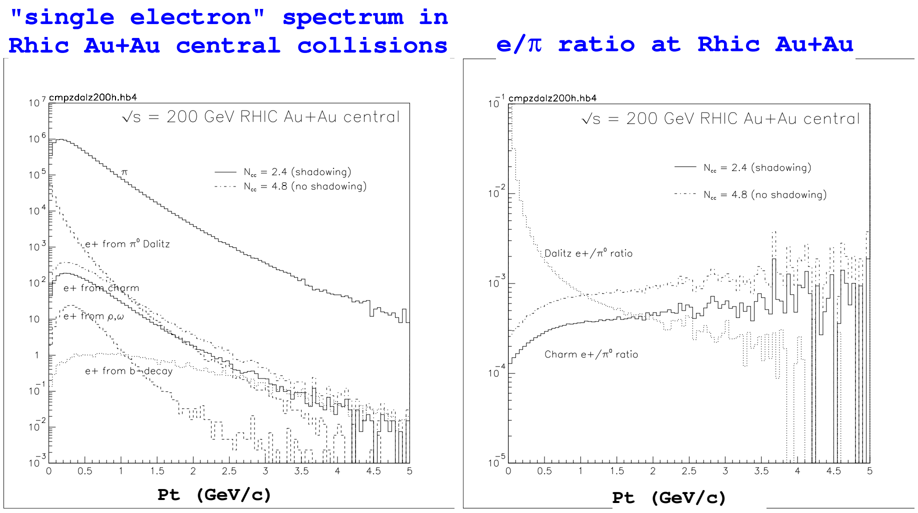

Figure 13: The contributions to the single electron transverse momentum spectrum, as compared to pions (left hand side), and the resulting e/pi ratio (right hand side), as calculated in Ref. [18], for no shadowing ($N_{\rm cc} = 4.8$) and shadowing ($N_{\rm cc} = 2.4$).

by Table 1. However, extracting the physics components of the spectrum will be a challenging task, even after a like-sign subtraction to remove the uncorrelated background. Two different techniques will help isolate the charm contribution: First, as emphasized by Tannenbaum[23], the production of single electrons at large transverse momenta is dominated by charm decays. The work of Akiba[18] shown in Figure 4.6 demonstrates the sensitivity of the e/π ratio for $p_T >\sim 1.5$ GeV/c to the charm yield, and thus to the nuclear shadowing. A second approach relies on PHENIX's capability for measuring $e-\mu$ coincidences (some hint of the rates may be obtained by comparing panels a, b and c of Figure 4.6). Since the first method does not have a combinatoric background, while the second covers a much larger rapidity interval, taken together these techniques will provide us with an excellent handle on the systematics inherent in any such measurement. Finally, it should be noted that the all-important shadowing of the gluon structure functions in nuclei may be measured directly in PHENIX using charm yields from p-A collisions, as recently suggested by Lin and Gyulassy[22].

5 Conclusions

The flexibility of the RHIC accelerator complex combined with the breadth of the PHENIX detector provides a unique facility for performing both first-generation "discovery" experiments as well as second-generation "characterization" measurements. There is no doubt that many surprises are in store; both in the first year of operation and the many years of physics that will follow.

Acknowledgments

It is a pleasure to acknowledge the extensive contributions of my many PHENIX colleagues to this work, as well as useful conversations with S. Gavin, M. Gyulassy, Z. Lin, K. Rajagopal, R. Vogt and X. Yang. The kind support of Prof. T. Kodama and the Centro Brasileiro de Pesquisas Fisicas is very much appreciated. This work was supported by the United States Department of Energy Grant DOE-FG02-86ER-40281.

1. For a review of recent work in the field, see *Proceedings of Quark-Matter '97* (Thirteenth International Conference on Ultra-Relativistic Nucleus-Nucleus Collisions), Tsukuba, Japan, December 1-5, 1997 (to appear in Nucl. Phys. A).
2. The most up-to-date information concerning the PHENIX experiment may be found at *http://www.rhic.bnl.gov/phenix/*.
3. Here *channel* refers to the observation of a particular final-state particle (e.g., electrons), as distinct from *signals* (e.g., enhancement of the e^+e^- pair-mass spectrum in the continuum below the ρ).
4. See "Spin Physics at RHIC", by M.J. Tannenbaum, in the Proceedings of *RHIC Summer Study '96*, July 8-19, 1996, D.E. Kahana and Y. Pang, eds., and "The PHENIX Spin Program", by N. Saito, in *Proceedings of QM97, ibid.*
5. For a review of recent work, see "The Chiral Phase Transition in QCD", by K. Rajagopal, in *Quark-Gluon Plasma 2*, edited by R. Hwa, World Scientific, 1995.
6. A. Breakstone *et al.* , Phys. Lett. **B135**, 510 (1984).
7. B.A. Cole, X.N. Wang, private communications.
8. *The PHENIX Conceptual Design Report*, 29-Jan-93.
9. T. Awes, private communication.
10. X.N. Wang, in the proceedings of this workshop.
11. *Photons and Lepton Pairs– The Deep Probes of the Quark-Gluon Plasma*, P.V. Ruuskanen, NATO Advanceed Study Institute on Particle Production in Highly Excited Matter, Lucca, Italy, July 1992.

12. *Physics from Photon and Di-Lepton Spectra*, G.R. Young, NATO Advanceed Study Institute on Particle Production in Highly Excited Matter, Lucca, Italy, July 1992.
13. *PHENIX CDR Update*, Nov-93.
14. The most current information regarding the EmCal and its performance may be found at *http://www.rhic.bnl.gov/phenix/WWW/emcal/emcal.html*.
15. M. Gyulassy and M. Plumer, Phys. Lett. **B243**, 432 (1990).
16. Xin-Nian Wang, Zheng Huang, and Ina Sarcevic, Phys. Rev. Lett. **77**, 231 (1996).
17. M. Leitch, private communication.
18. Y. Akiba, in *Physics with the Collider Detectors at RHIC and the LHC, Proceedings of the Pre-Conference Workshop*, Quark Matter '95, Monterey, CA, J. Thomas and T. Hallman, eds., UCRL-ID-121571, pp. 131-142 (1995).
19. S.Gavin *et al.* , Phys. Rev. **C54**, 2606 (1996).
20. B. Muller and X.N. Wang, Phys. Rev. Lett. **68**, 2437 (1992).
21. K. Geiger, Phys. Rev. **D48**, 4129–4145 (1993).
22. Z. Lin and M. Gyulassy, Phys. Rev. Lett. **77**, 1222–1225 (1996).
23. *Charm in PHENIX– a signal or a background?*, M.J. Tannenbaum, to appear in Heavy Ion Physics.